

CONFIDENTIAL

Copy
RM E54L24

b

UNCLASSIFIED



RESEARCH MEMORANDUM

CORRELATION OF VIBRATORY ROOT FAILURES
AND STRESS DISTRIBUTION IN J65
COMPRESSOR BLADES

By André J. Meyer, Jr., and Albert Kaufman

Lewis Flight Propulsion Laboratory
Cleveland, Ohio

CLASSIFICATION CHANGED

To UNCLASSIFIED

By authority of HPA # 17 *Officed.* Date 3/18/60
95 H

CLASSIFIED DOCUMENT

This material contains information affecting the National Defense of the United States within the meaning of the espionage laws, Title 18, U.S.C., Secs. 793 and 794, the transmission or revelation of which in any manner to an unauthorized person is prohibited by law.

NATIONAL ADVISORY COMMITTEE FOR AERONAUTICS

WASHINGTON

September 8, 1955

CONFIDENTIAL

UNCLASSIFIED

NACA RM E54L24



NATIONAL ADVISORY COMMITTEE FOR AERONAUTICS

RESEARCH MEMORANDUM

CORRELATION OF VIBRATORY ROOT FAILURES AND STRESS DISTRIBUTION

IN J65 COMPRESSOR BLADES

By André J. Meyer, Jr., and Albert Kaufman

SUMMARY

The stress distribution in the roots of the first three stages of the J65 axial-flow compressor was determined in order to explain root failures experienced in service. The failures are apparently the result of the combination of vibratory stresses and stresses due to centrifugal force, particularly the high bending stresses in the serration fillets caused by the serration teeth performing as short, highly loaded cantilever beams. High vibratory stresses alone could not be made to produce failures, but in conjunction with simulated centrifugal loads, root failures could be readily produced in the laboratory.

On the basis of the information gained, changes in the root proportions are proposed and the stress distribution for the new designs are presented. Without changing the contour or rim thickness of the standard J65 rotor disks, the vibration stresses in the root are reduced 55 percent by the proposed design; the centrifugal and gas bending stresses are reduced 27 percent. The shear stresses through the serration teeth are approximately the same for the two root profiles.

INTRODUCTION

The J65 steel-bladed engine has experienced a number of first-stage compressor-blade failures in service. The failures are the result of the blade vibrations and consistently occur in the second serration of the blade root. Stress analysis of the fir-tree-type roots of the first three stages of the compressor (the most critical stages from the vibration aspect) was undertaken to determine if it was possible to eliminate failures by redesigning the roots. The engine manufacturer is also investigating root forms from other engines for which broaches are available as a means of improving root design. The program reported herein is an attempt to approximate the optimum form obtainable with the space limitations of conventional rotors without being limited to existing broaches.

Vibration measurements during normal engine operation are being made under a separate investigation. The maximum vibratory stresses observed on the airfoils in these tests to date were used in the calculations. Also test blades were subjected to fatigue at these same and higher stress levels.

As a result of the stress computations and the experimental program, a new root design is proposed for the first three stages of the axial-flow compressor. An analytical and experimental comparison between the strength of the original and the new designs is presented.

COMPUTATIONS AND DISCUSSION

Stress Computations on Standard J65 Blade Roots

The necessary information for computing the stresses was obtained from manufacturing drawings. The pertinent dimensions are tabulated in table I and the basic root profiles are shown in figure 1. The vibratory stresses measured in the engine are listed in the following paragraph.

Vibratory stresses. - Resistance-wire strain gages were applied on each side of the airfoil as close to the platform of the blade as possible. They were cemented at the thickest point along the camber line of the airfoil-base cross section. At this location the maximum stresses observed in the engine thus far and corresponding engine speeds as reported in reference 1 are:

Stage	Maximum vibratory stress, psi	Speed, rpm
1	±26,400	5182
2	±26,160	5860
3	±16,140	6060

These stresses are the result of first-bending-mode vibrations of the airfoil. Of more importance for this investigation, are the vibratory stresses actually existing in the root, but they are inaccessible to direct measurement. Using the simple basic equation for bending stress gives

$$S = \frac{Mc}{I}$$

where

S outside fiber stress, psi

5386

- M bending moment, lb in.
- c distance from neutral axis to outside fiber, in.
- I moment of inertia of cross section in question, in.⁴

988C
CF-1 back

The vibratory stresses in the base can be crudely approximated. First, after S, c, and I at the cross section of the strain-gage location are known, the moment M producing the vibratory stress can be determined. The moment consists of the product of the vibratory force and the distance from the gage location to the point where this force can be assumed to be concentrated. By placing a series of strain gages along the span of a vibrating cantilever beam, it was found that the vibratory stress in the lower 15 percent of the beam was linearly proportional to the distance from the tip. The actual point of application of the exciting force along the cantilever span was varied, but the position of application had very little effect on the resultant stress distribution in the base region. This result is to be expected, since the shape of the deflection curve of a vibrating cantilever beam is not appreciably affected by exciting force location. The deflection curve is primarily determined by the distribution of inertia forces along the blade span, which is established by the blade geometry. Consequently, to determine the stress at any point near the base, a concentrated load apparently can be assumed to be acting at the blade tip. When the distances from the gage to the tip of the blade and also from the serration necks to the blade tip are known, the moment acting at the serrations because of the hypothetical concentrated load can be estimated; and with c and I known for the respective serration necks, the vibratory stresses in the root can be approximated.

With the fir-tree arrangement, it is impossible to determine accurately where and how the blade is restrained with respect to the bending forces of the vibrations, and it is undoubtedly different for every blade in the rotor. The worst condition would result when the blade is restrained by bearing against only the serration tooth just below the neck for which the stress is computed. This condition is unrealistic, because a single pair of serrations is incapable of retaining the whole blade. The loaded pair of teeth would deform until more teeth engaged. A more realistic assumption would be to consider an equal distribution of the vibratory stresses carried by each of the four pairs of serrations. In this case the bottom serrations would carry only one-fourth the stress that would exist when the bottom serrations tried to carry the whole load, the other three-fourths being removed to the wheel by the three upper pairs of serrations. The third set of serrations would carry half the vibratory stress for the worst condition, that of the third serrations being the only serrations engaged. This stress would be due to the load carried by the bottom serrations combined with the vibratory load removed to the compressor rotor by the third pair. Similarly, the second serrations would carry three-quarters and the top serrations would carry the whole vibratory load. The estimated vibratory stresses using these assumptions are tabulated as follows:

████████████████████

Serration	Stage		
	1	2	3
1	11,470	9630	5510
2	12,140	11,471	6570
3	11,590	12,830	7360
4	8950	12,800	7350

These stress magnitudes without additional factors are insufficient to cause failure in the root. In fact, the airfoil stresses are higher than the root stresses for the second serration where failures are occurring and should result in airfoil failures were it not for the higher stress-concentration factors in the root.

Stress concentrations. - The reason failures take place in the root and not in the airfoil is detectable in figure 1. The fillets at the base of the serrations are much smaller (0.0125 and 0.0245-in. rad.) than the fillet (0.188-in. rad.) at the airfoil and platform junction. Furthermore, the airfoil fillet is a 90° fillet compared with 45° notches in the lower three serrations, and this further reduces the stress concentration at the airfoil fillet.

The theoretical stress-concentration factors in accordance with Neuber's equations for bending (ref. 2) for the serration notches and from reference 3 for the airfoil fillets have been determined and are as follows:

	Stage	
	1	2 and 3
Airfoil	1.18	1.13
Serration 1	2.38	2.32
Serration 2	2.95	2.81
Serration 3	2.79	2.59
Serration 4	2.60	2.30

These stress-concentration factors should be adjusted by sensitivity factors (ref. 4) taking into account the material properties, surface

finish, and size effect. Sensitivity factors, however, are extremely variable and differ greatly depending on their source. Since reliable sensitivity factors can only be obtained by extensive fatigue testing of the part in question, they are not included here.

The vibratory stresses multiplied by their respective stress-concentration factors are:

	Stage		
	1	2	3
Airfoil	31,150	29,560	18,240
Serration 1	27,330	22,320	12,760
Serration 2	35,840	32,270	18,490
Serration 3	32,360	33,190	19,040
Serration 4	23,280	29,460	16,920

From this table it can be seen that the vibratory stress is greater in the second serration of the first-stage rotor blade than anywhere else.

To obtain a complete picture of the stress distribution of the blade, the centrifugal and gas bending loads must be determined.

Centrifugal stresses. - The centrifugal stresses throughout the airfoil of the blade can be readily determined if the cross-sectional areas are known at several stations along the span of the blade (ref. 5). The centrifugal stresses in the serration necks can also be calculated by first computing the mass of the blade, platform, and sections of the root. The simplifying assumption that the total centrifugal load is divided equally among the serrations must be made, since the exact distribution cannot be determined and it differs between blades.

The centrifugal-stress distribution for the three blades at the rated speed of the engine (8300 rpm) is plotted graphically in figure 2. For other speeds, the stress at any point can be proportioned directly according to the square of the speed. The stresses at the main points of interest for both rated speed and the speed where the maximum vibrations were observed for each stage, respectively, are given in table II.

Gas bending stresses. - The gas forces acting on the individual blades were approximated by the procedure used in the appendix of reference 6. It was necessary to assume that each compressor stage did an

equal amount of work and that the work load per stage was divided equally among the blades of the stage. The resultant stresses due to gas forces considered to be acting at the center of pressure are listed in table II. These stresses were computed for rated-speed conditions.

Summation of stresses. - The steady-state and vibratory stresses cannot be added algebraically, but their effects can be accumulated by modified Goodman diagrams (ref. 7). The gas bending stresses at rated speed are relatively small. At the speeds where the maximum vibration amplitudes were observed, they are reduced 57 to 76 percent and therefore become relatively unimportant. The fatigue endurance limit of the blade material (no. 403 Austenitic stainless steel) varies according to hardness and with a measured hardness of Rockwell 108-B is 75,000 pounds per square inch (fig. 3). A Goodman diagram for the J65 blade is given in figure 4. From the figure it is apparent that the computed vibratory, centrifugal, and gas bending stresses combined cannot account for the failure. The highest combined mean working stress under vibration conditions for the three stages considered is 14,280 pounds per square inch (13,200 psi centrifugal stress plus 1080 psi gas bending stress, third stage, first serration, table II). From the diagram, the maximum working stress would then be 82,400 pounds per square inch, which means that the maximum allowable vibratory stress is 68,100 pounds per square inch (82,400 minus 14,280). Obviously, other less apparent forces and their resultant stresses are contributing to the failures since the maximum computed vibratory root stress including stress concentration factor is 35,840 pounds per square inch.

When the vibrating blade reaches the maximum deflection point, the bearing loads due to centrifugal force and the vibratory moment are much higher on the serrations on one side of the root than on the other (fig. 5). In the next half of the vibration cycle the loading is reversed. These combined alternating bearing loads act on the serration teeth, which essentially perform as short cantilever beams to produce magnified tensile stresses along the fillet at the upper surface of the tooth. Because the loads are alternating, the fillet tensile stresses are subject to stress-concentration effects. To determine the magnitude of these stresses with reasonable accuracy is very difficult. First, the load distribution over the bearing surface is indeterminate and differs with each tooth. And secondly, the stress distribution in such an extremely short cantilever with rapidly changing cross section is practically impossible to calculate analytically. The problem could possibly be solved by photoelasticity for an ideal loading condition, but the true fatigue life of the blade can be determined more easily and more reliably by experimental fatigue tests.

Fatigue Tests on Original J65 Blade Roots

To establish the fatigue life of the J65 compressor blades and to observe locations of failure, several blades were pneumatically vibrated at their first-bending-mode natural frequency in the apparatus illustrated in figure 6. Air is impinged on the tip of a blade which has been mounted in a standard rotor disk. Strain gages, located in the same position as the gages in the engine, are used occasionally to measure vibration stresses. Slight adjustments in air pressure are made to maintain a constant stress amplitude.

Initially the blades merely were inserted tightly in the conventional disk. These blades were vibrated with an airfoil stress up to $\pm 33,000$ pounds per square inch for over 10^8 cycles without failure, or at 25 percent over the maximum stress observed in the engine. This result confirmed the conclusion that failure could not be produced with the computed vibratory stresses alone. Next the disk was drilled and threaded to permit simulating the centrifugal force by tightening hardened cap screws against the bottom of the root. The total centrifugal load of each blade acting on the root fastening in the first three stages is about 4800 pounds at the engine speed where the vibration amplitudes are a maximum. By utilizing a universal tensile testing machine, a torque of 190 inch-pounds on each of two one-quarter inch diameter cap screws was found necessary to duplicate this desired load. With the cap screws tightened to this torque, the blades could be failed in fatigue at airfoil vibratory stresses as low as $\pm 21,000$ pounds per square inch (fig. 7). A typical failure is photographed in figure 8. The final break repeatedly occurred across the second serration similar to the engine failures. Consistently, however, the earliest indications of failure during these tests (apparent from a decrease in the blade natural frequency) was evidenced by a cracking of the first serration. These initial cracks did not progress tangentially across the first-serration neck, nor radially along the shear plane of the tooth. The cracks propagated diagonally downward to the fillet of the second-serration neck and then tangentially across the neck between the second pair of serrations. The first crack is the result of the combination of the vibratory, the simulated centrifugal, and the high cantilever bending stresses mentioned in the preceding section. The cracks cause much higher stress-concentration factors at the second-serration fillet than computed in table I. Furthermore, all stresses acting on the remaining serrations are increased when the first serration is no longer capable of carrying any load. In an engine or in a rotating test rig, the evidence of the origin of failure is lost but it is probable that the mechanism of failure is similar.

Redesigned Blade Root to Reduce Vibration-Failures

Examination of the fir-tree root of the standard J65 compressor blades shows that the serration fillets are smaller than necessary.

By using three pairs of larger serrations instead of four pairs of small serrations, the fillet radii can be greatly increased with no increase in shear stresses.

Also, the computed centrifugal stresses in the rotor segments between adjacent blade roots are much lower than similar stresses in the blade roots and are lower than necessary (see table II). Apparently the blade-serration necks can be widened and the rotor-serration necks can be reduced and thus greatly increase the over-all strength of the root-fastening assembly.

Several root configurations for the J65 blades have been designed and stress analyzed until the most suitable compromise between all factors concerned was approached. Particular attention was given to increasing the bending stiffness of the individual serration teeth. The included tooth angle was increased from 45° for the original root to 60° for the new design. The final proportions selected are profiled in figure 9. Two different profiles are presented for the first stage. One has the same cross section and thus could be made with the same broach as needed for stages 2 and 3. The other design, slightly more efficient, is suggested for the first stage if still greater strength warrants the cost of separate broaches. Root forms other than fir-tree styles were considered, but repeatedly the stress distribution was found to be less favorable. Also two pair-of-serrations fir-tree arrangements were investigated and, even though much larger fillets could be used, the net resultant stresses were higher than those determined for the profiles presented in figure 9. The pertinent dimensions of these root forms are listed in table I and the computed stresses given in table II.

A four-pair-of-serrations root form can be designed which is stronger than the proposed three serration root; but to provide large fillets, the root must penetrate deeper radially into the rotor. The radial thickness of the rotor rim would therefore have to be increased and may in turn require a thicker disk to carry the heavier rim load. It is doubtful that the advantage in root strength could offset the disadvantage of increased engine weight.

A comparison of the different stresses between the original root design for the J65 compressor and the new proposals is made in the following sections.

Vibratory stresses. - Because the serration necks are wider in the proposed blade root, the moments of inertia opposing the vibratory bending forces are larger (table I) and, consequently, the vibratory stresses are lower. For the same computed forces acting in the engine, the root stresses due to vibrations are:

	Stage			
	1	2	3	1a
Serration 1	7680	5440	3110	4920
Serration 2	8190	5830	3340	5390
Serration 3	7450	5320	3060	5140

Comparing these values with those in the table at the top of page 4 shows that an average reduction of about 50 percent has been effected. This is without the influence of stress-concentration factors.

Stress concentrations. - Increasing the serration neck distances slightly increases the stress-concentration factors; however, this effect is more than offset by the large increases in fillet radii. The theoretical stress concentrations for the proposed root proportions are as follows:

Stage	1, 2, and 3	1a
Serration 1	2.359	2.495
Serration 2	2.205	2.334
Serration 3	2.015	2.126

An average decrease of 14 percent is the result of the change in root design (compare with table at the bottom of p. 4). Combining this improvement with the reduction in vibratory stresses shows a total average decrease of 55 percent in the effective vibratory stresses in the serrations. The alternating bending stresses at the fillet from the serration teeth acting as cantilevers are similarly reduced as the stress-concentration factor decreases.

Centrifugal and gas bending stresses. - Because of the increased neck distances between blade serrations, the centrifugal and gas bending stresses are reduced as can be seen by comparing like stresses for the old and new design in table II. The highest centrifugal stress in the original root is 25,800 pounds per square inch and is in the first-stage blade. This stress was reduced 27 percent or to 18,700 pounds per square inch for the new design.

These improvements were accomplished at the expense of the centrifugal stresses in the rotor segment between adjacent blades. The highest rotor stress formerly was 17,300 pounds per square inch, while

the new design raises this level to 24,750 pounds per square inch, still a conservative value.

In a new design, however, the shear and the bearing stresses should be determined.

Shear stresses. - As shown in table II, the shear stresses in both the blade and the rotor teeth of the new design are about the same as in the original design. To ascertain if a sufficient margin of safety exists, a number of 1/8-inch-diameter pin specimens were subjected to double shear. The shear strength as determined for the blade material was 65,910±500 pounds per square inch. Thus, the safety factor is almost 3, which is more than ample. The wheel material was not checked; however, the operating shear stresses are lower in the wheel than in the blade and, therefore, unquestionably the wheel has a sufficient margin of safety.

Bearing stresses. - The bearing stresses for both root designs are also tabulated in table II, the computed values show an increase of 27.6 percent as a result of the root changes. An increase in bearing stresses may be desirable to assure more uniform load distribution between serration teeth. It is unlikely that the bearing-stress increase will be detrimental; but if lower bearing stresses are desired, they can be accomplished by decreasing the serration apex radius on the blade root, however, this will increase the tensile stresses in the wheel serrations and will also decrease the shear stresses in the wheel serrations.

Experimental Evaluation of Root Designs

To fabricate the proposed root designs from stainless steel and to machine a wheel segment with serrations from a conventional disk material for fatigue testing would involve prohibitive expenditures. As the second best alternative, enlarged profile models were routed from a methyl methacrylate plastic. These models of the three different root forms were subjected to increasing loads in bending until fracture occurred. Because the plastic material has low ductility and therefore is notch sensitive, it simulates the behavior of ductile blade materials under fatigue conditions. Fracture loads of the plastic models are thus indicative of the relative fatigue strengths of the various root designs. The average fracture loads, relative strength ratios, and theoretical strength ratios in bending are:

Root	Fracture load, lb	Load ratio	Theoretical ratio
Original	1134	1:1	1:1
Proposed	1599	1.41:1	1.49:1
Alternative proposal	2357	2.08:1	2.21:1

Although the experimental strength ratios are lower than theoretically predicted values, agreement is sufficiently close to induce confidence in the computations. Of special significance is the fracture of the model of the original root form. As shown in figure 10, the break occurred primarily across the second serration neck although the top tooth also broke away similar to the fractures experienced in the fatigue tests.

CONCLUSIONS

Several simplifying assumptions were made in the computations; however, the same assumptions were used in determining the comparative stresses of both designs. Therefore, although the quantitative magnitude of the stress values may be of questionable accuracy, the qualitative comparison should be reliable.

Fatigue tests and calculations indicated that the cause of root failure was primarily the high alternating bending stress of the serration tooth acting as a short, heavily loaded cantilever beam. The vibratory stresses measured in blades along with the computed tensile stress due to the centrifugal force and gas load were not sufficient to produce failure.

For identical vibratory forces acting on the airfoil, the effective vibratory stress in the roots is reduced 55 percent by the proposed root design changes. Further, the centrifugal tensile and gas bending stresses in the roots are reduced 27 percent, which permits a slightly higher vibratory stress to exist in the root before failure occurs. The reduction of 14 percent in stress-concentration factors likewise reduces the cantilever bending stresses of the root, which are also alternating as an effect of the vibrating action of the blade.

These improvements were accomplished with an increase in the maximum centrifugal stress in the wheel segment between blades. The increase still produces conservative stresses in the wheel because initially the wheel stresses were unnecessarily low. The shear stresses are essentially the same for both designs and the bearing stresses are increased 28 percent by the redesign. The change in root design suggested can be made without changing the shape or size of the wheel blanks. The proposed root designs should, therefore, help to eliminate root fatigue failures in the J65 axial-flow compressor without introducing new root problems.

Lewis Flight Propulsion Laboratory
National Advisory Committee for Aeronautics
Cleveland, Ohio, December 21, 1954

REFERENCES

1. Calvert, Howard F., Braithwaite, Willis M., and Medeiros, Arthur A.: Rotating-Stall and Rotor-Blade-Vibration Survey of a 13-Stage Axial-Flow Compressor in a Turbojet Engine. NACA RM E54J18, 1955.
2. Neuber, H.: Theory of Notch Stresses: Principles for Exact Stress Calculation. Trans. No. 74, David Taylor Model Basin, Nov. 1945.
3. Hartman, J. B., and Leven, M. M.: Factors of Stress Concentration for the Bending Case of Fillets in Flat Bars and Shafts with Central Enlarged Sections. Proc. Soc. Exp. Stress Analysis, vol. IX, no. 1, 1951, pp. 53-62.
4. Maleev, V. L.: Machine Design. International Textbook Co., 1946, pp. 75-98.
5. Kemp, Richard H., and Morgan, William C.: Analytical Investigation of Distribution of Centrifugal Stresses and Their Relation to Limiting Operating Temperatures in Gas-Turbine Blades. NACA RM E7L05, 1948.
6. Meyer, A. J., Jr., Deutsch, G. C., and Morgan, W. C.: Preliminary Investigation of Several Root Designs for Cermet Turbine Blades in Turbojet Engine. II - Root Design Alterations. NACA RM E53G02, 1953.
7. Noll, G. C., and Lipson, C.: Allowable Working Stresses. Proc. Soc. Exp. Stress Analysis, vol. III, no. 2, 1946, pp. 89-101.

TABLE I. - J65 ROOT DIMENSIONS AND GEOMETRIC PROPERTIES

Stage	Serration	Blade					Rotor			
		Radius, in.	Neck Width, in.	Neck area, sq in.	Neck moment of inertia, in. ⁴	Stress concentration factor	Neck width, in.	Neck area, in.	Radius, in.	Stress concentration factor
Original design										
1	1	0.0245	0.384	0.450	5.526×10^{-3}	2.383	0.534	0.626	0.0175	3.121
	2	.0125	.325	.381	3.362	2.953	.576	.676		3.214
	3	.0125	.273	.321	1.998	2.792	.615	.721		3.263
	4	.0125	.222	.260	1.065	2.600	.657	.771		3.311
2	1	0.0245	0.353	0.333	3.461×10^{-3}	2.318	0.444	0.420	0.0175	2.860
	2	.0125	.282	.267	1.770	2.813	.498	.471		2.971
	3	.0125	.219	.207	.831	2.586	.550	.520		3.045
	4	.0125	.156	.148	.301	2.301	.600	.567		3.114
3	1	0.0245	0.353	0.337	3.501×10^{-3}	2.318	0.476	0.455	0.0175	2.860
	2	.0125	.282	.270	1.791	2.813	.528	.505		2.971
	3	.0125	.219	.210	.841	2.586	.581	.554		3.045
	4	.0125	.156	.150	.305	2.301	.634	.606		3.114
Proposed design - Same profile										
1	1	0.0313	0.4671	0.5479	9.962×10^{-3}	2.359	0.426	0.500	0.0230	2.575
	2	.0313	.3737	.4384	5.102	2.205	.485	.569		2.678
	3	.0313	.2803	.3288	2.153	2.015	.543	.637		2.768
2	1	0.0313	0.4671	0.4414	8.025×10^{-3}	2.359	0.300	0.284	0.0230	2.301
	2	.0313	.3737	.3531	4.109	2.205	.372	.352		2.466
	3	.0313	.2803	.2649	1.734	2.015	.444	.420		2.608
3	1	0.0313	0.4671	0.4465	8.118×10^{-3}	2.359	0.328	0.314	0.0230	2.369
	2	.0313	.3737	.3573	4.158	2.205	.402	.384		2.528
	3	.0313	.2803	.2680	1.755	2.015	.475	.454		2.662
Proposed design - Alternative										
1	1	0.0313	0.5842	0.6853	19.490×10^{-3}	2.495	0.331	0.388	0.0230	2.364
	2	.0313	.4608	.5405	9.564	2.334	.445	.522		2.590
	3	.0313	.3374	.3958	3.755	2.126	.558	.655		2.765

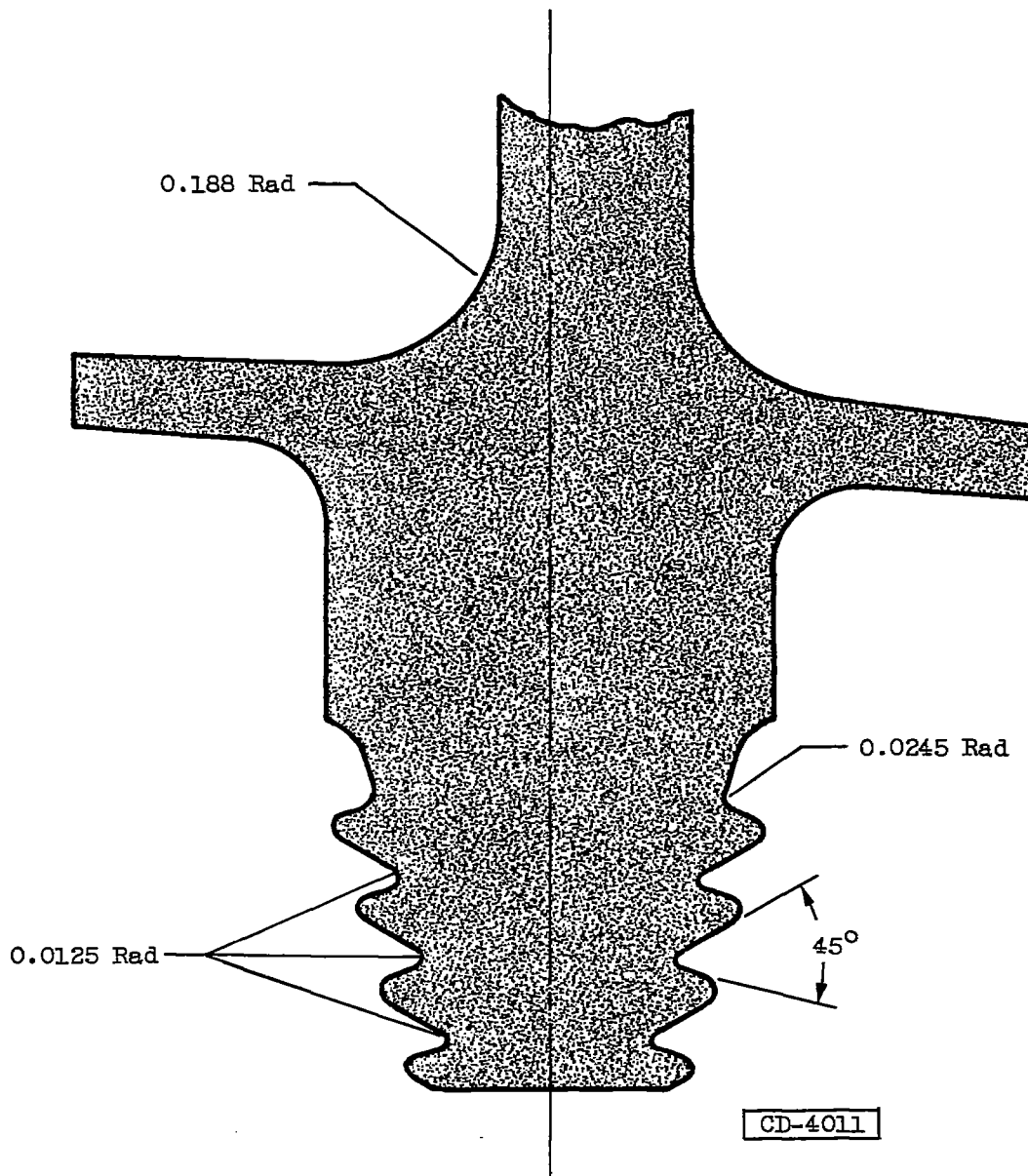
TABLE II. - J65 ROOT STRESSES FOR ORIGINAL AND PROPOSED DESIGNS

14

Stage	Serration	Blade root stresses, psi							Rotor stresses, psi			
		Centrifugal stress		Gas bending stress at rated speed	Shear stress	Bearing stress	Vibratory stress	Vibratory stress times concentrations	Centrifugal stress		Shear	Bearing
		Rated speed	Speed of maximum vibration						Rated speed	Speed of maximum vibration		
Original design												
1	1	25,800	10,050	3550	26,250	61,200	11,470	27,330	5,400	2,100	23,000	61,200
	2	23,350	9,100	4000			12,140	35,640	9,650	3,760		
	3	18,900	7,350	3880			11,590	32,360	13,500	5,250		
	4	12,050	4,700	3000			8,950	23,280	17,300	6,750		
2	1	24,600	12,250	3090	21,350	60,080	9,630	22,520	5,800	2,900	18,200	60,100
	2	23,700	11,800	3740			11,471	32,270	9,750	4,850		
	3	20,900	10,400	4080			12,830	33,190	13,450	6,700		
	4	15,150	7,550	4240			12,800	29,460	16,500	8,250		
3	1	24,750	13,200	2510	21,850	61,480	5,510	12,760	5,550	2,950	18,650	61,500
	2	23,900	12,750	3050			6,570	18,490	9,550	5,100		
	3	21,150	11,250	3520			7,360	19,040	13,150	7,000		
	4	15,350	8,200	3340			7,350	18,920	15,900	8,500		
Proposed design - Same profile												
1	1	21,200	8,250	2390	24,100	66,000	7,680	18,120	9,000	3,500	21,440	66,000
	2	18,500	7,200	2600			8,190	18,060	18,350	7,150		
	3	13,100	5,100	2410			7,450	15,010	21,500	8,400		
2	1	18,800	9,250	1910	21,550	72,650	5,540	12,830	11,400	5,700	19,180	72,650
	2	16,450	8,200	2090			5,830	12,880	18,300	9,100		
	3	11,800	5,900	1950			5,320	10,720	23,550	11,750		
3	1	18,700	9,950	1540	21,850	74,550	3,110	7,340	8,450	4,500	19,450	74,550
	2	16,850	8,900	1700			3,340	7,360	17,250	9,200		
	3	12,000	6,400	1590			3,060	6,170	24,750	13,200		
Proposed design - Alternative												
1	1	16,950	6,600	1530	26,700	91,500	4,920	12,280	11,750	4,600	21,440	91,500
	2	15,200	5,800	1720			5,390	12,580	17,100	6,650		
	3	11,100	4,350	1670			5,140	10,930	21,000	8,200		

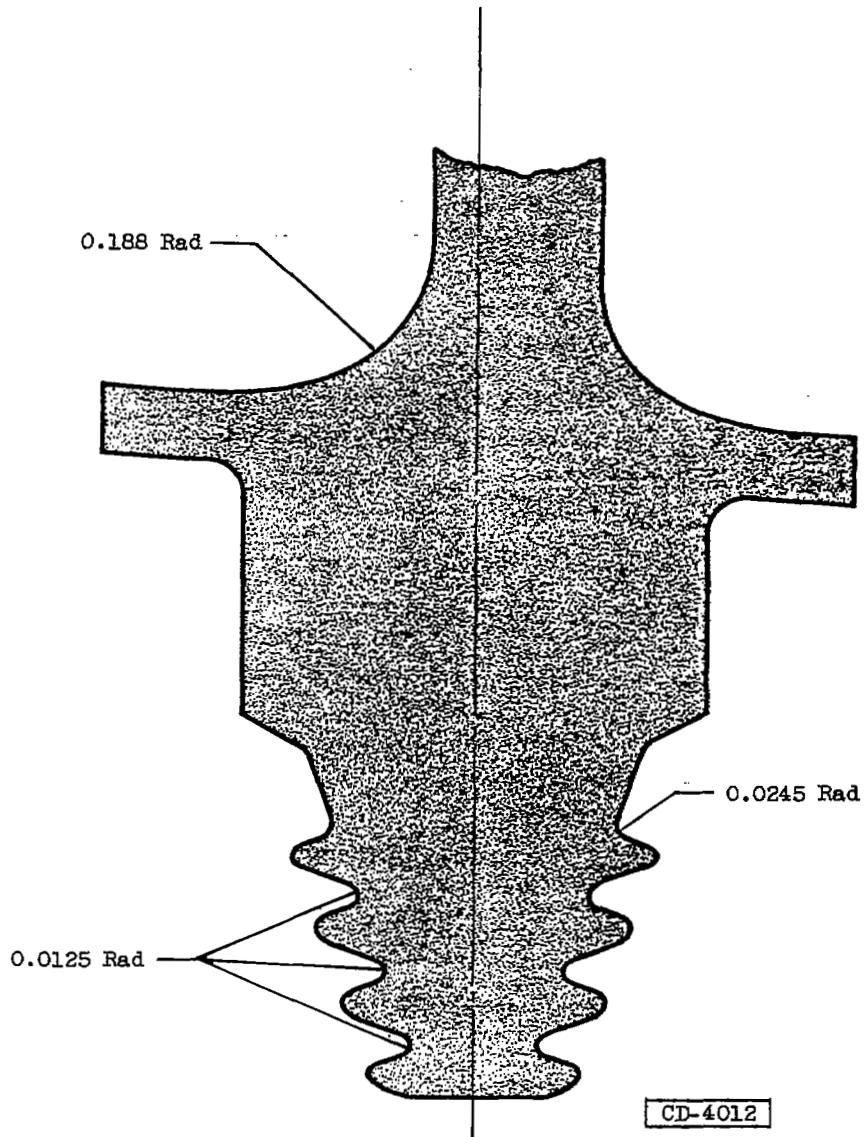
NACA RM E54124

3386



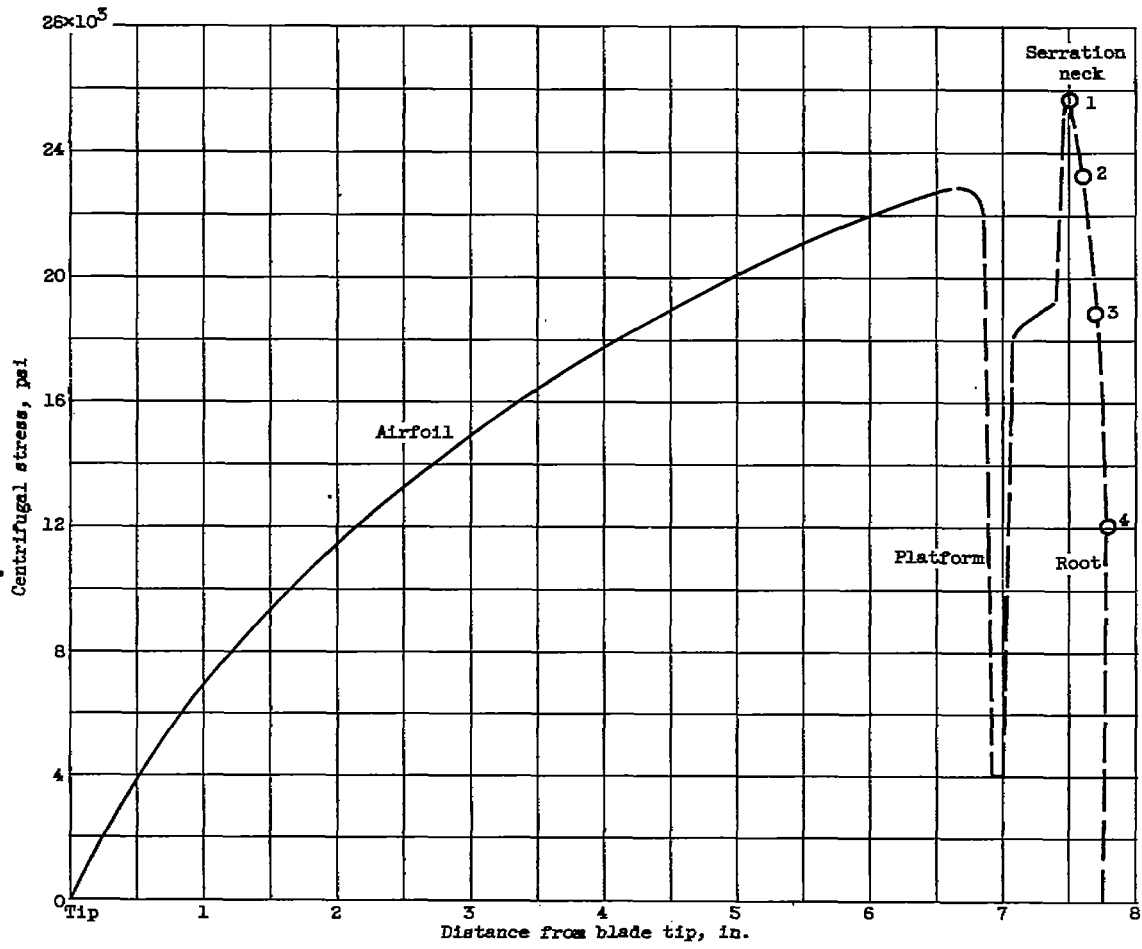
(a) First-stage blade.

Figure 1. - Standard J65 root profiles. (All dimensions are in inches.)



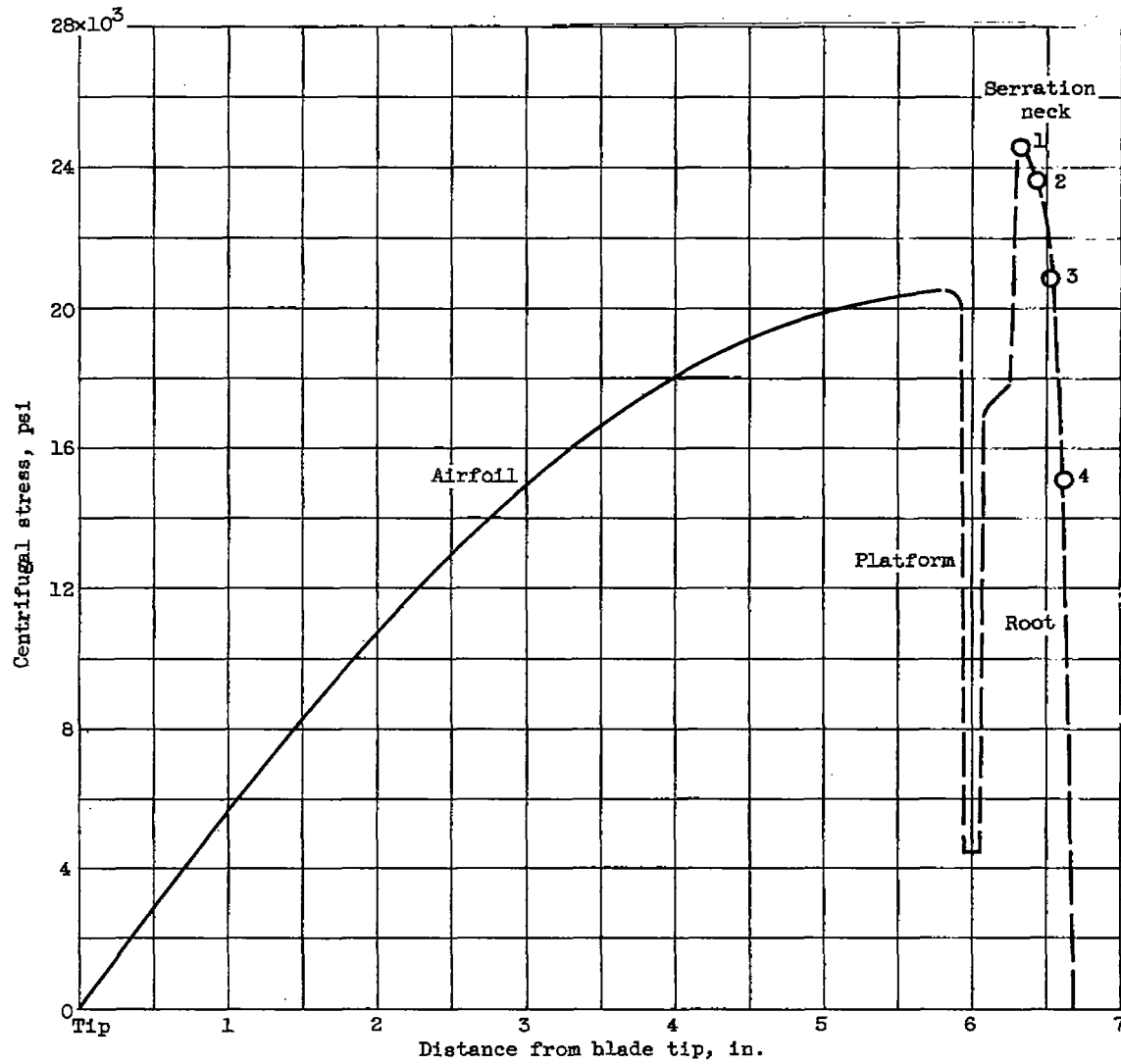
(b) Second- and third-stage blades.

Figure 1. - Concluded. Standard J65 root profiles. (All dimensions are in inches.)



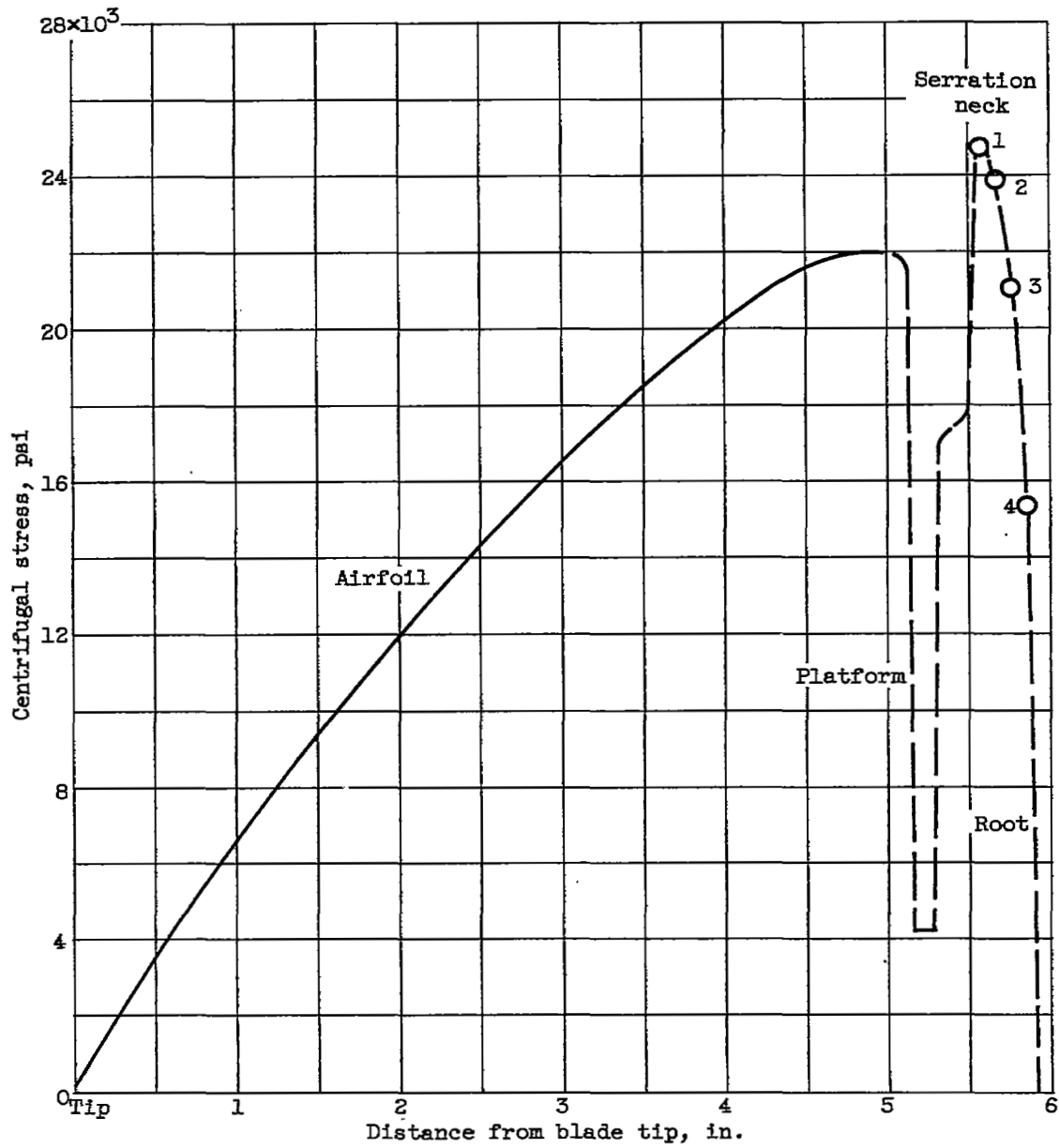
(a) First-stage blade.

Figure 2. - Centrifugal-stress distribution throughout airfoil span and in standard root.



(b) Second-stage blade.

Figure 2. - Continued. Centrifugal-stress distribution throughout airfoil span and in standard root.



(c) Third-stage blade.

Figure 2. - Concluded. Centrifugal-stress distribution throughout airfoil span and in standard root.

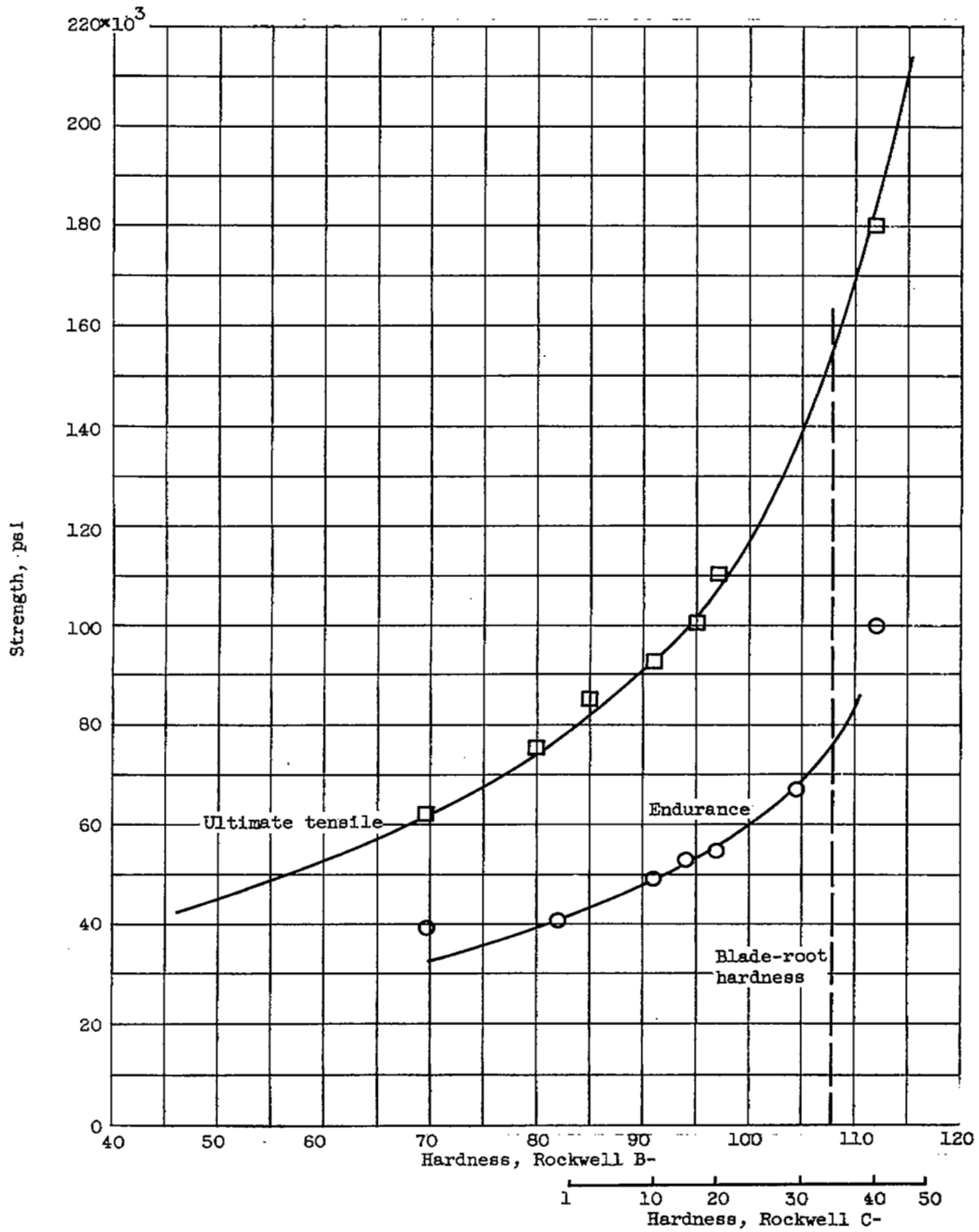


Figure 3. - Mechanical properties of 403 stainless steel.

3386

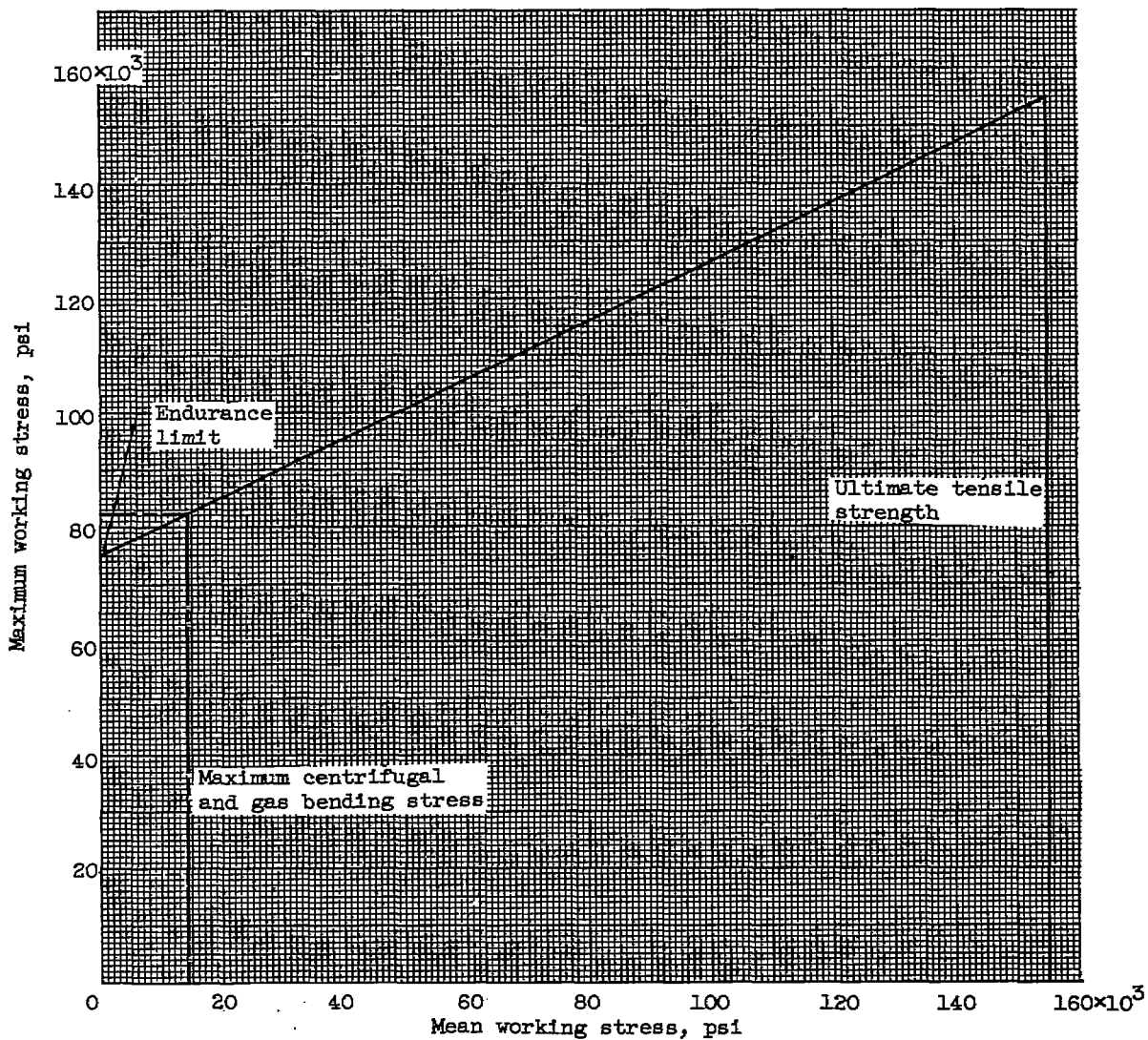
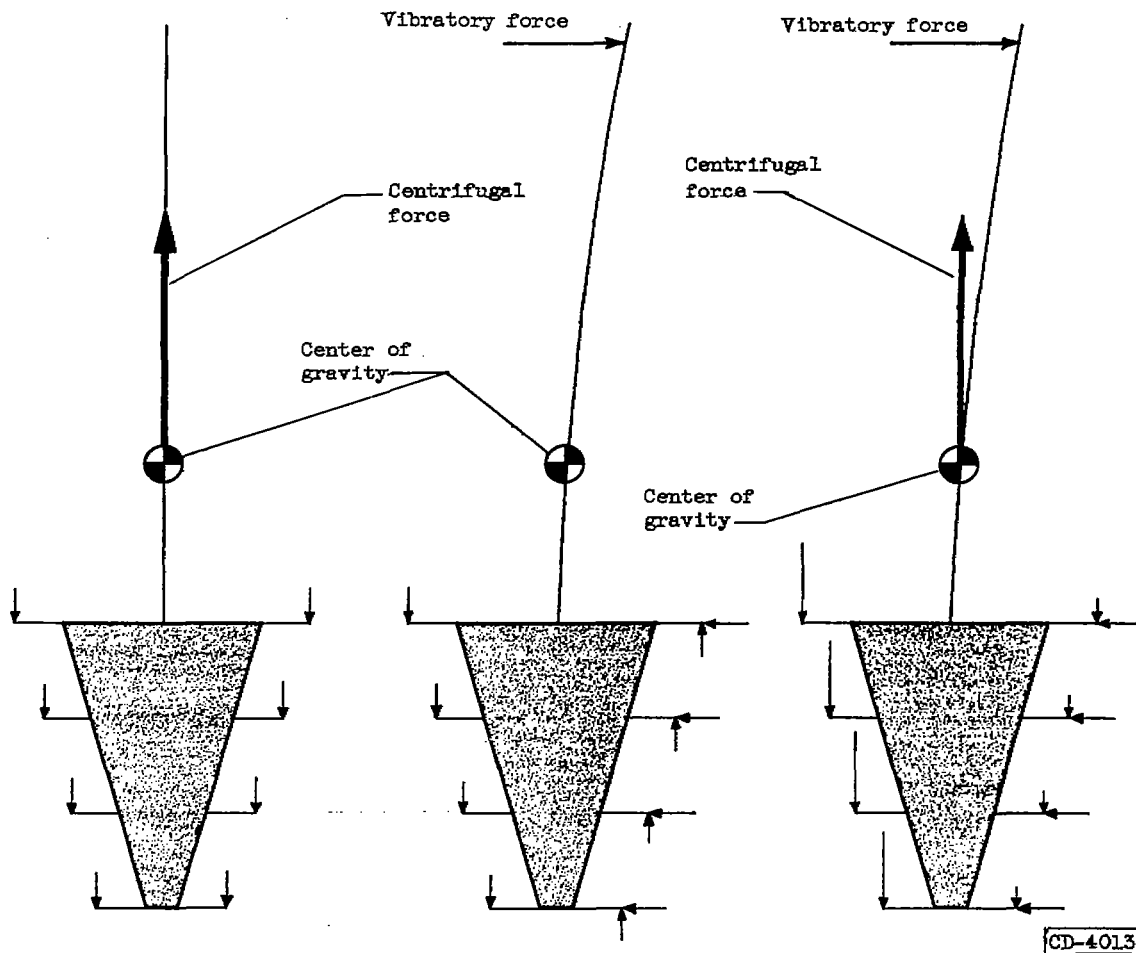


Figure 4. - Modified Goodman diagram for 403 stainless steel blade material.



(a) Centrifugal loads.

(b) Vibratory loads.

(c) Combined centrifugal and vibratory loads.

Figure 5. - Schematic diagram of forces acting on blade with and without vibratory forces.

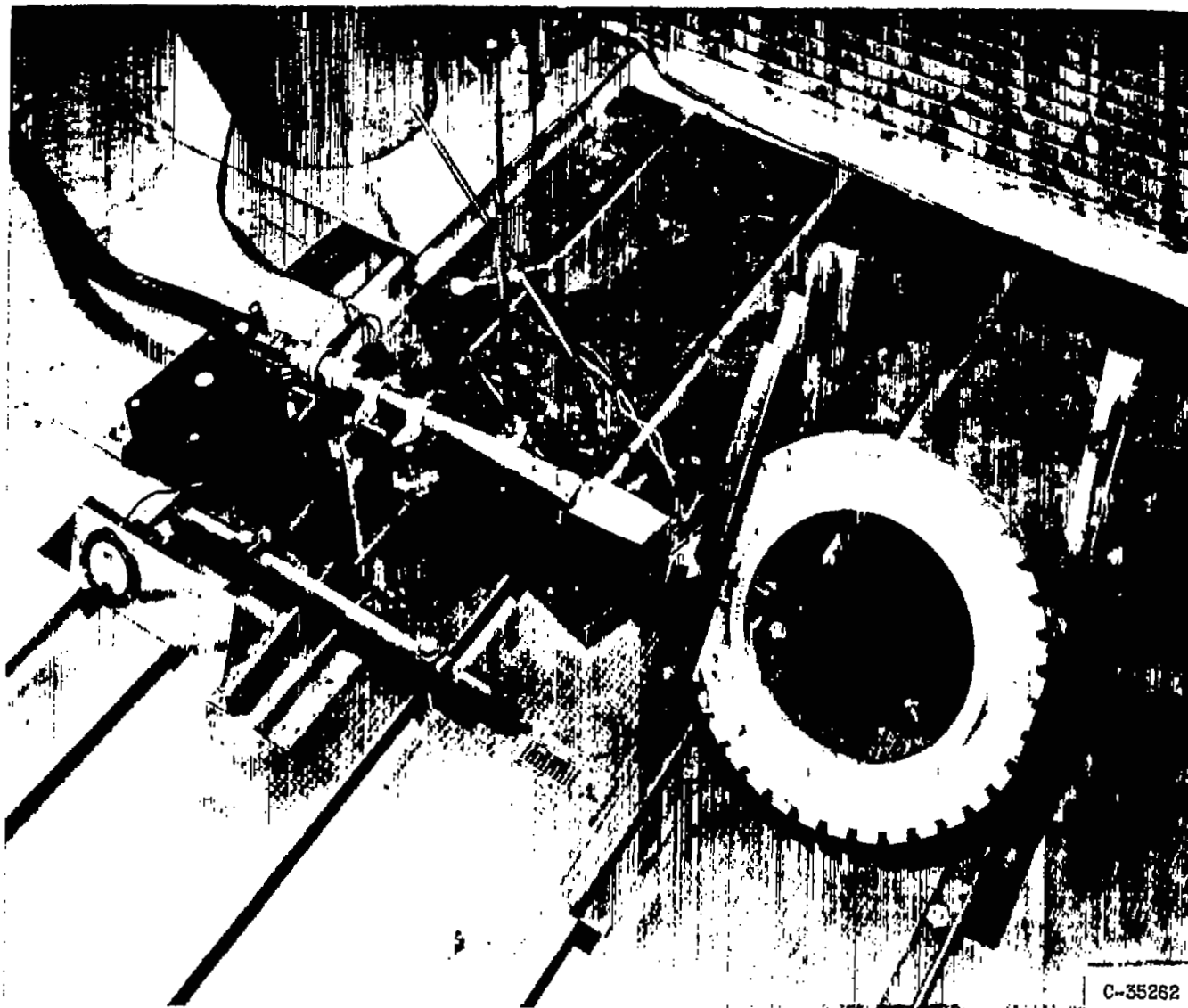


Figure 6. - Apparatus used for fatiguing standard J65 blades.

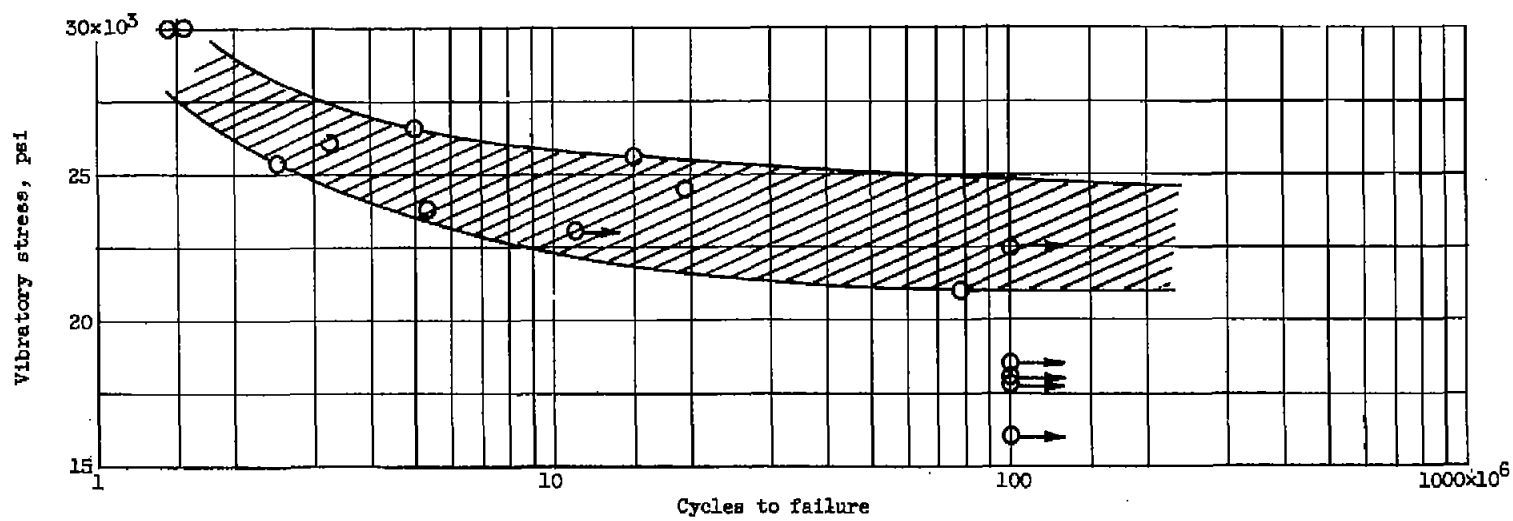
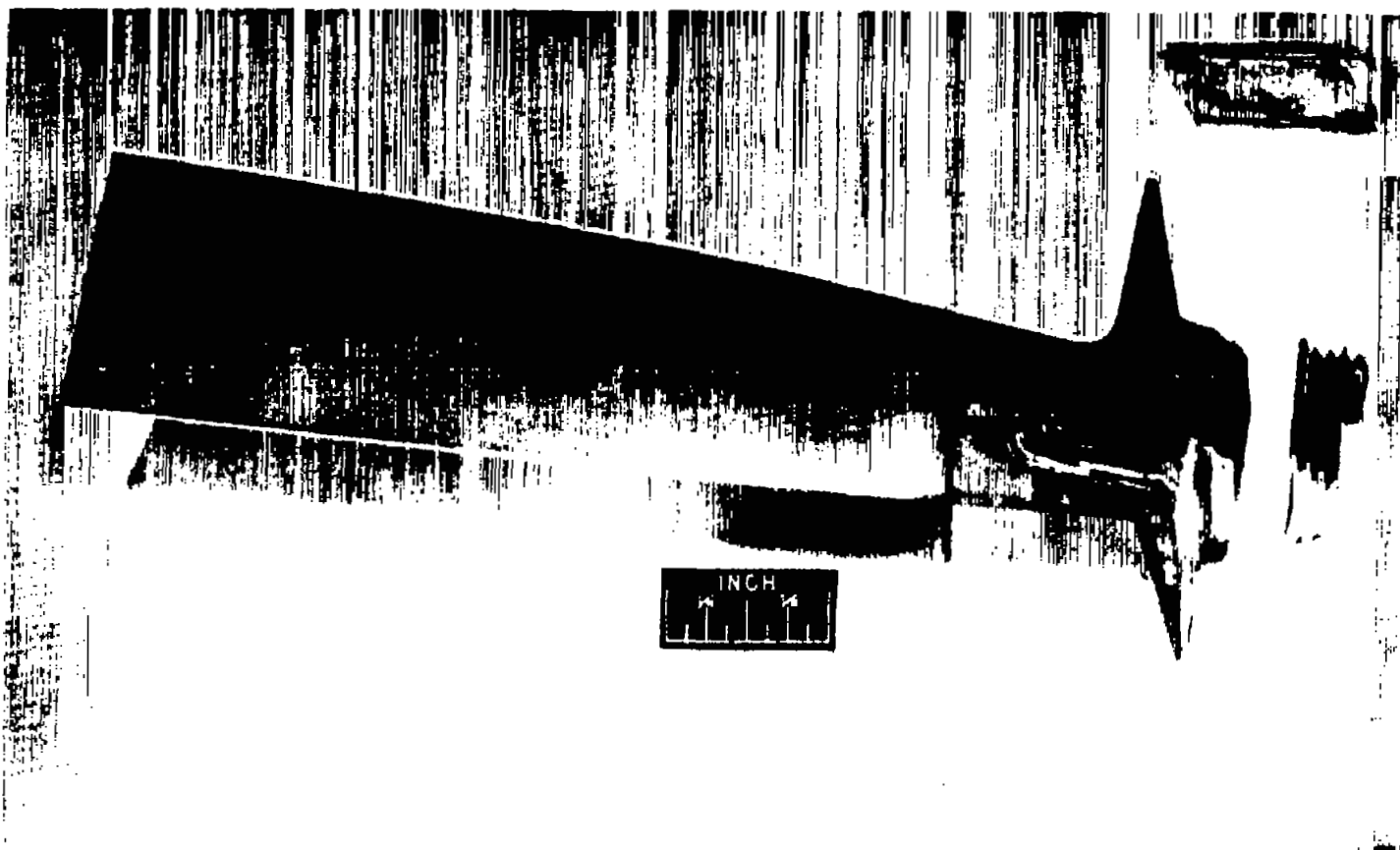
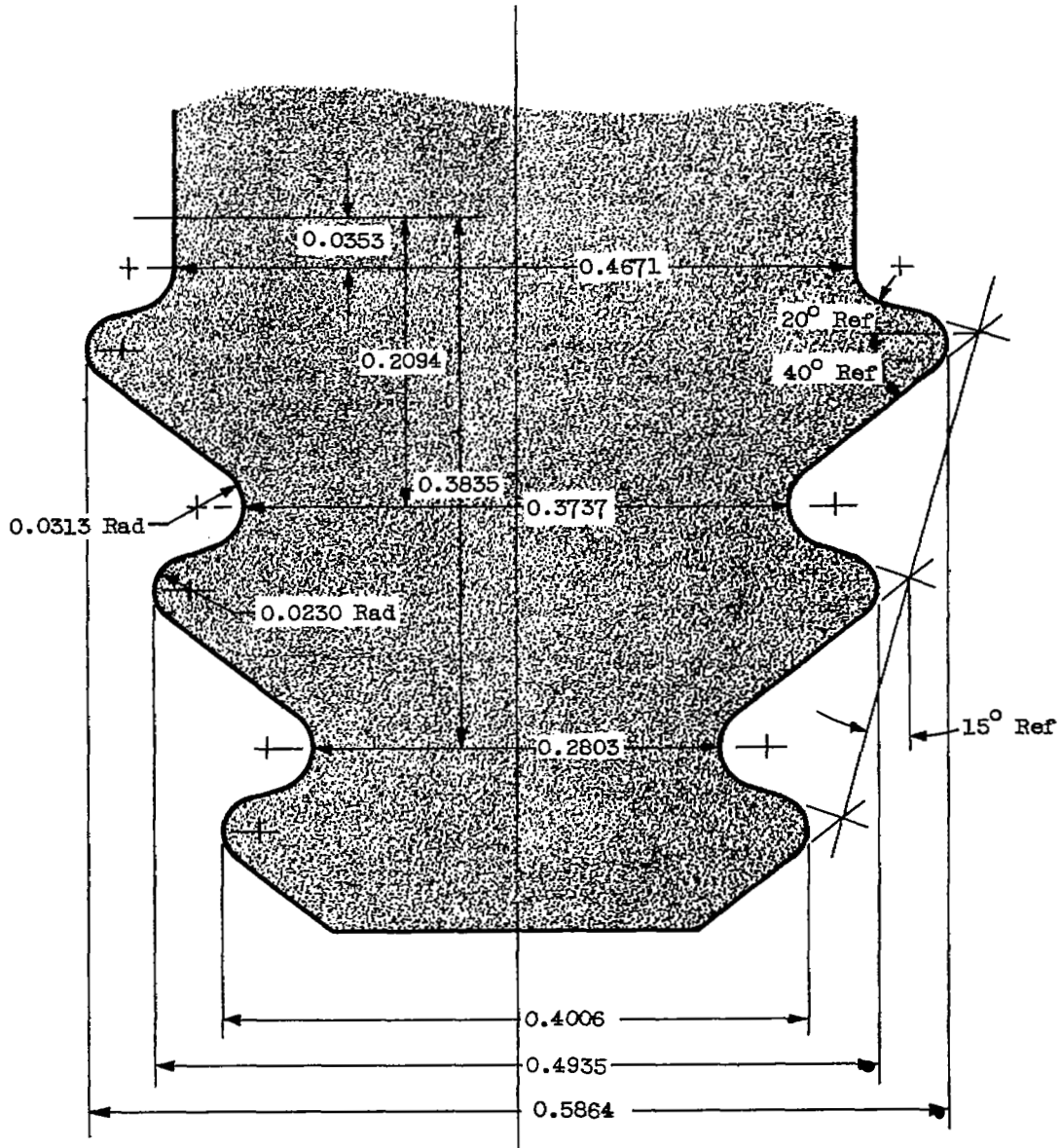


Figure 7. - Results of fatigue tests of standard J65 blades.



C-35085

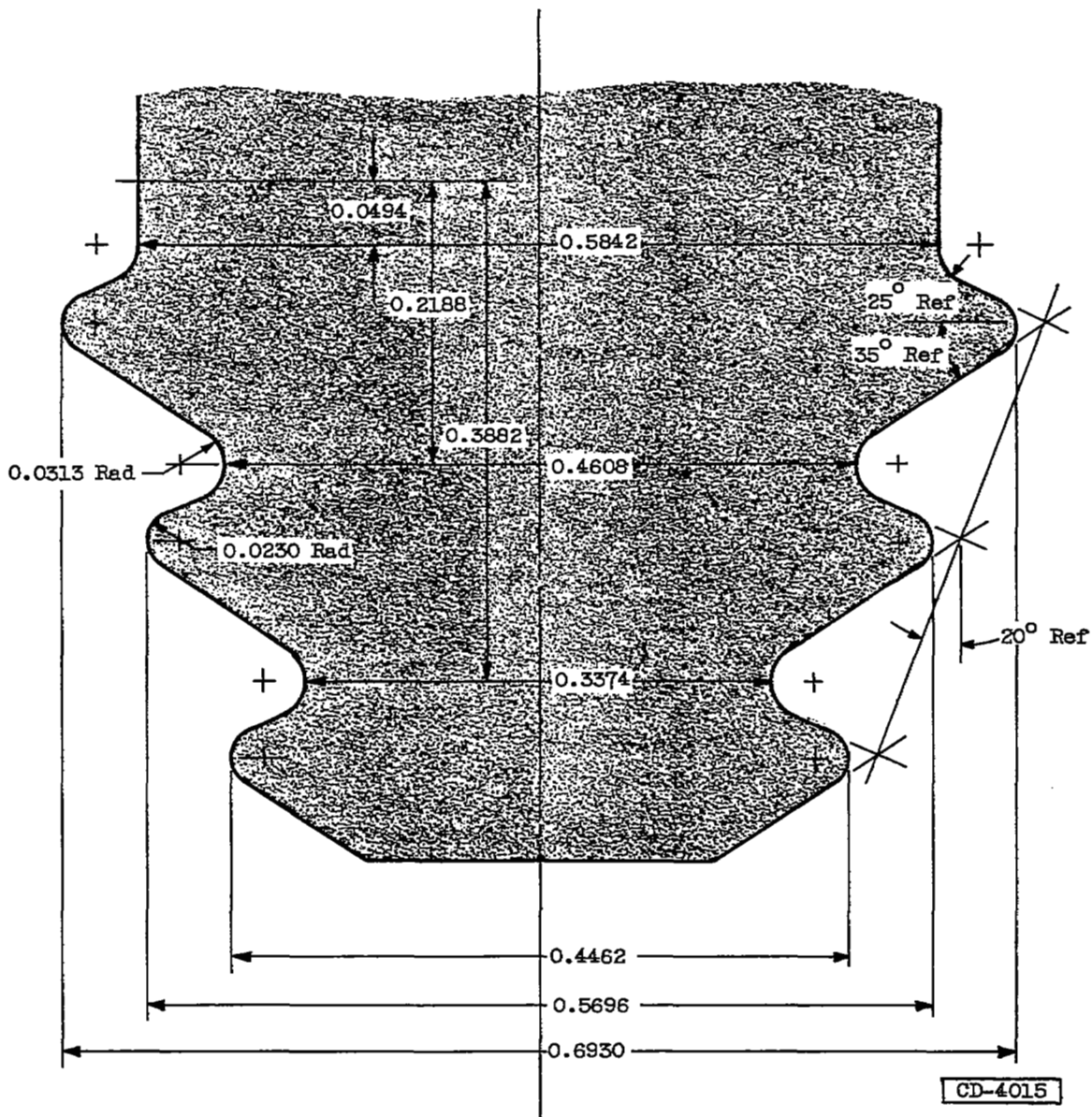
Figure 8. - Typical J65 compressor-blade failure.



CD-4014

(a) First three stages.

Figure 9. - Proposed root profiles for J65 compressor rotor blades. (All dimensions are in inches.)



(b) Alternate design for first stage.

Figure 9. - Concluded. Proposed root profiles for J65 compressor rotor blades.
 (All dimensions are in inches.)

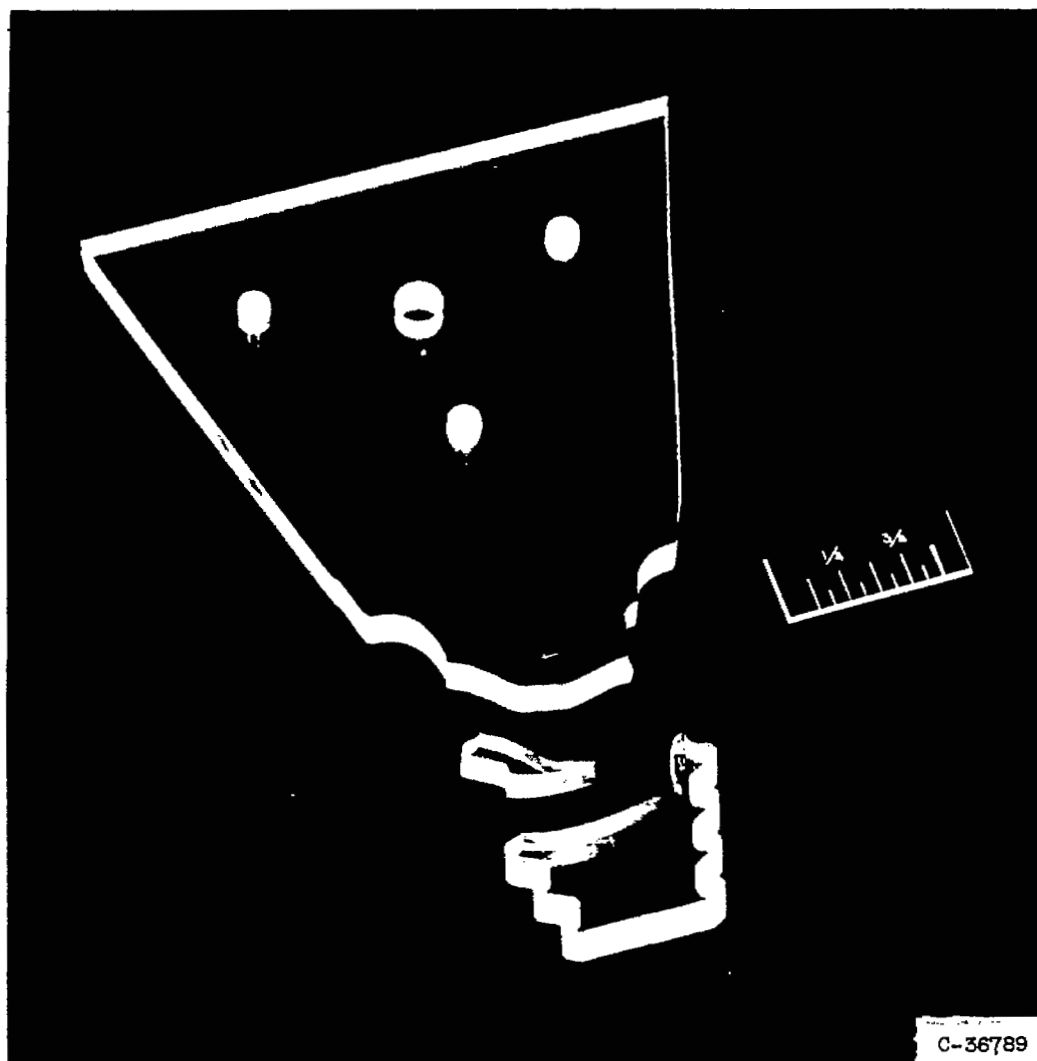


Figure 10. - Typical failure of plastic model.

NASA Technical Library



3 1176 01435 7868

